



Contents lists available at ScienceDirect

Biochemical and Biophysical Research Communications

journal homepage: [www.elsevier.com/locate/ybbrc](http://www.elsevier.com/locate/ybbrc)

## Structure of the GH1 domain of guanylate kinase-associated protein from *Rattus norvegicus*



Junseon Tong<sup>a</sup>, Huiseon Yang<sup>a</sup>, Soo Hyun Eom<sup>b</sup>, ChangJu Chun<sup>a,\*</sup>, Young Jun Im<sup>a,\*</sup>

<sup>a</sup> College of Pharmacy, Chonnam National University, Gwangju 500-757, South Korea

<sup>b</sup> School of Life Sciences, Steitz Center for Structural Biology, and Department of Chemistry, Gwangju Institute of Science and Technology, Gwangju 500-712, South Korea

### ARTICLE INFO

#### Article history:

Received 6 August 2014

Available online 22 August 2014

#### Keywords:

Protein structure

X-ray crystallography

Synaptic scaffolding protein

GKAP

Protein–protein interaction

Helix bundle

### ABSTRACT

Guanylate-kinase-associated protein (GKAP) is a scaffolding protein that links NMDA receptor-PSD-95 to Shank–Homer complexes by protein–protein interactions at the synaptic junction. GKAP family proteins are characterized by the presence of a C-terminal conserved GKAP homology domain 1 (GH1) of unknown structure and function. In this study, crystal structure of the GH1 domain of GKAP from *Rattus norvegicus* was determined in fusion with an N-terminal maltose-binding protein at 2.0 Å resolution. The structure of GKAP GH1 displays a three-helix bundle connected by short flexible loops. The predicted helix  $\alpha 4$  which was not visible in the crystal structure associates weakly with the helix  $\alpha 3$  suggesting dynamic nature of the GH1 domain. The strict conservation of GH1 domain across GKAP family members and the lack of a catalytic active site required for enzyme activity imply that the GH1 domain might serve as a protein–protein interaction module for the synaptic protein clustering.

© 2014 Elsevier Inc. All rights reserved.

### 1. Introduction

Synaptic function depends on proper localization of various ion channels, receptors, and signalling molecules in the synapse. Targeting of these molecules is mediated by their interactions with specific intracellular anchoring or clustering proteins [1]. The post-synaptic density (PSD) is an electron-dense structure associated with the cytoplasmic face of the postsynaptic membrane. The PSD consists of a network of proteins that link glutamate receptors and other postsynaptic proteins to the cytoskeleton and signalling pathways in the excitatory synapses [2]. GKAPs (also known as Discs, large-associated protein 1, DLGAP1) are a family of scaffold proteins initially identified by their interaction with the guanylate kinase (GK) domain of postsynaptic density protein 95 (PSD-95) [3]. GKAP facilitates the assembly of the post synaptic density of neurons by interacting with various binding partners such as synaptic scaffolding molecule [4], Shank [5], dynein light chains [6], disks large homolog 1 [7]. By these interactions, GKAP physically links the N-methyl-D-aspartic acid (NMDA) receptor-PSD-95 complex to the type I metabotropic glutamate receptor-Homer complex and to motor proteins [8].

There are at least six alternative splicing variants of GKAP in *Rattus norvegicus* and seven variants in humans [3]. GKAP family proteins are characterized by the presence of a GKAP homology domain 1 (GH1) of 160 amino acids in the C-terminal region of these proteins [1,3]. The longest isoform in rat, GKAP1 is composed of 992 amino acids. The N-terminal 800 residues are predicted to be unstructured, while the C-terminal GH1 domain is predicted to be composed of four or five  $\alpha$ -helices. GKAP binding to Shank proteins is mediated by a short C-terminal PDZ binding sequence common to all GKAP splice variants [5]. GKAP binding to the GK domain of PSD-95 is mediated by the N-terminal region containing multiple 14 amino acid repeats conserved in all GKAP proteins [3].

Regulation of synaptic protein clustering by GKAP is dynamic. Stimulating neuronal activity induces the ubiquitination and degradation of GKAP and Shank, while inactivity induces synaptic accumulation of GKAP [9,10]. The biochemical changes at synapses accompanied by chronic activity modulation by the ubiquitin-proteasome system provide a potential molecular mechanism for homeostatic plasticity [10]. Still, the molecular mechanisms of GKAP regulation on the post-synaptic targeting and remodelling of proteins in the PSD are largely unknown.

The GKAP GH1 has no recognizable similarity to any characterized protein domains and has no sequence homology to the proteins of known structures in the Protein Data Bank. However, conservation of this region across the GKAP homologs and the presence of predicted  $\alpha$ -helical structures indicate that the GH1

\* Corresponding authors.

E-mail addresses: [chun1130@jnu.ac.kr](mailto:chun1130@jnu.ac.kr) (C. Chun), [imyounjung@jnu.ac.kr](mailto:imyounjung@jnu.ac.kr) (Y.J. Im).

domain may represent a discrete domain with a functional significance.

In order to obtain a structural insight into the role of GKAP GH1, we determined the crystal structure of GKAP homology domain 1 from *R. norvegicus* and examined the biochemical properties by isothermal titration calorimetry. The structure of the GKAP GH1 displays a three-helix bundle which associates weakly with the helix  $\alpha 4$ . This work provides a structural platform for the study on the function of the conserved GKAP GH1 domain.

## 2. Materials and methods

### 2.1. Cloning, protein expression and purification

Details of construct design, protein preparation and crystallographic procedures were described elsewhere [11]. Briefly, DNA encoding the C-terminal GH1 domain (residues 807–971) of GKAP (UniProt ID P97836) was amplified by polymerase chain reaction (PCR) using a cloned GKAP DNA from *R. norvegicus*. The PCR product was subcloned into the *NcoI* and *XhoI* sites of a modified pHis-parallel2 vector. GKAP was tagged with an N-terminal hexahistidine followed by a thrombin protease cleavage site (LVPR/GS). To improve the crystallization property of the GKAP construct, 29 residues (residues 917–945) in the flexible  $\alpha 3$ – $\alpha 4$  loop were replaced by a dipeptide sequence (Val-Asp) of the *Sall* restriction enzyme recognition sequence by PCR based mutagenesis. The PCR product amplified from the pHis-GKAP GH using the primers, 50-CTAGATAGTCGACCGCTCGCTGGAGAGCTC-30 (sense) and 50-CTAGATAGTCGACCTGTTTCAATTATTGG-30 (antisense) was digested with *Sall* restriction enzyme. Then, the digested DNA was self-ligated to generate the loop truncation. Open reading frames of all mutant genes were confirmed by DNA sequencing.

To produce a fusion construct of His-tagged MBP (maltose-binding protein) and GKAP, DNA of the loop truncated GKAP GH1 was subcloned into the *NcoI* and *XhoI* sites of the modified pHis-MBP vectors. The MBP (UniProt ID P0AEX9) was modified to lack the last nine residues in the C-terminal  $\alpha$ -helix compared to wild type MBP. The N-terminus of GKAP was connected to the modified MBP (residue 1–387) with a two-amino acid linker originating from the *NcoI* recognition sequence. The modification of MBP was designed to minimize the flexibility of the connecting loop between MBP and GKAP. The pHis-MBP-GKAP GH1 (residues 807–971, 917–945 $\Delta$ ) was transferred into *Escherichia coli* strain BL21(DE3) cells. Transformed cells were grown to an OD<sub>600</sub> of 0.8 at 310 K in Luria-Bertani medium and protein expression was induced by the addition of 0.25 mM isopropyl  $\beta$ -D-1-thiogalactopyranoside. The culture was incubated for 12 h at 293 K before harvesting cells. Cells expressing His-MBP-GKAP GH1 were resuspended in lysis buffer (2 $\times$  PBS buffer supplemented with 30 mM imidazole) and lysed by sonication. Cell lysates were centrifuged at 13,000 rpm for 45 min. The supernatant containing His-MBP-GKAP was applied to a Ni-NTA affinity column. The Ni-NTA column was thoroughly washed with the lysis buffer. The protein was eluted from the column using 0.1 M Tris-HCl pH 7.0, 0.3 M imidazole, 0.3 M NaCl. The eluate was concentrated to 10 mg/ml and the His-tag was removed by cleavage with thrombin protease. MBP-GKAP GH1 was subjected to size-exclusion chromatography on a Superdex 200 column (GE Healthcare) equilibrated with 20 mM Tris-HCl pH 7.5, 0.1 M NaCl. The fractions containing MBP-GKAP were concentrated to 10 mg/ml for crystallization.

### 2.2. Crystallization and crystallographic analysis

Crystals of the MBP-GKAP GH were grown in 0.1 M sodium citrate pH 5.0, 15% PEG 1500, 0.1 M NaCl with a typical size

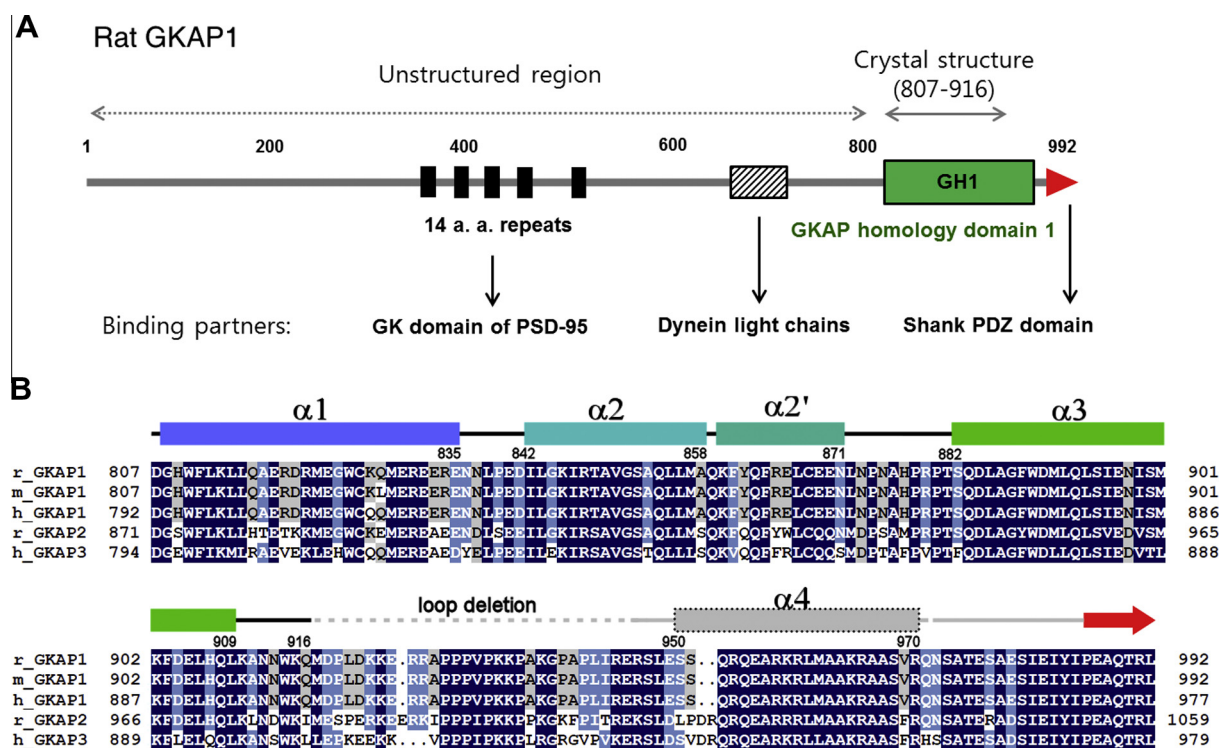


**Fig. 1.** Schematic presentation of GKAP and GH1 domain. (A) Schematic presentation of the domain structures of GKAP1 from *Rattus norvegicus*. The upstream sequences of GKAP GH1 domain were predicted to be mostly unstructured based on the secondary structure prediction (<https://www.predictprotein.org/>). (B) Sequence alignments of the GH1 domains of GKAP homologs (UniProt IDs, rat GKAP1: P97836, mouse GKAP1: Q9D415, human GKAP1: O14490, rat GKAP2: P97837, human GKAP3: O95886). Predicted secondary structure elements are indicated by dotted rectangles. Truncation of the  $\alpha 3$ – $\alpha 4$  loop is indicated by a dotted line. The PDZ binding motif is indicated with a red arrow. (For interpretation of the references to color in this figure legend, the reader is referred to the web version of this article.)

**Table 1**  
Summary of diffraction data statistics.

Crystal	MBP2-GKAP
Wavelength (Å)	0.97857
X-ray source	PLS-7A
Space group	$P2_12_12$
Unit cell	$a = 99.1 \text{ \AA}$ , $b = 158.7 \text{ \AA}$ , $c = 65.5 \text{ \AA}$
Resolution (Å) (last shell)	50–2.0 (2.03–2.00)
Observed number of reflections	469,641
No. of unique reflections	68,103 (2793)
Multiplicity	6.9 (3.9)
$I/\sigma(I)$	45.6 (3.9)
$R_{\text{merge}}$ (%)	7.6 (40.9)
Data completeness (%)	97.1 (80.5)
Phasing	MR (MBP)
Refinement (last shell)	50–2.0 (2.00–2.13)
$R_{\text{work}}/R_{\text{free}}$	0.243/0.281 (0.324/0.364)
R.m.s. bond length (Å)	0.006
R.m.s. bond angle ( $^\circ$ )	1.2
Average B value ( $\text{\AA}^2$ )	48.0
Number of atoms	7625 (water 181)

Values in parentheses are for the highest resolution shell.  
 $R_{\text{free}}$  is calculated for a randomly chosen 5% of reflections.

of  $0.2 \times 0.2 \times 0.1 \text{ mm}$  by micro-seeding techniques. The crystals were cryoprotected by transferring them into reservoir solution supplemented with an additional 10% PEG 1500 and 10% (v/v)

glycerol and were flash-cooled by immersion in liquid nitrogen. Diffraction data for MBP-GKAP crystals were collected at a wavelength of  $0.97857 \text{ \AA}$  using an ADSC Q270 CCD detector on the 7A beamline at Pohang Light Source (PLS), Pohang Accelerator Laboratory. All data were processed and scaled using *HKL-2000* (HKL Research Inc.) and handled with the *CCP4* program suite [12]. Molecular replacement using MBP structure (PDB id: 1OMP) was carried out using *MOLREP* [13].

The MBP fusion provided an additional advantage in determining phase information by molecular replacement. Two copies of MBP were found in the asymmetric unit using the MBP structure of an open conformation as a search model [14]. The phases were further improved by density modification using the program *CNS* [15] and the resulting electron density map with a figure of merit of 0.78 was readily interpretable. Two molecules of MBP-GKAP were clearly visible in the electron density maps. The structure of MBP-GKAP was built manually using the program *Coot* [16] and the structure was refined to  $R_{\text{work}}/R_{\text{free}}$  of 24.3%/28.1% using *CNS*. The final model consisted of two copies of MBP-GKAP (GKAP residues 807–906) and 181 water molecules. There are 95.4% of the residues in the most favored and additional allowed regions of the Ramachandran plot. Seven residues have conformations in disallowed regions, and all of these are the residues in the extreme termini of chains or in the loop regions of high flexibilities.

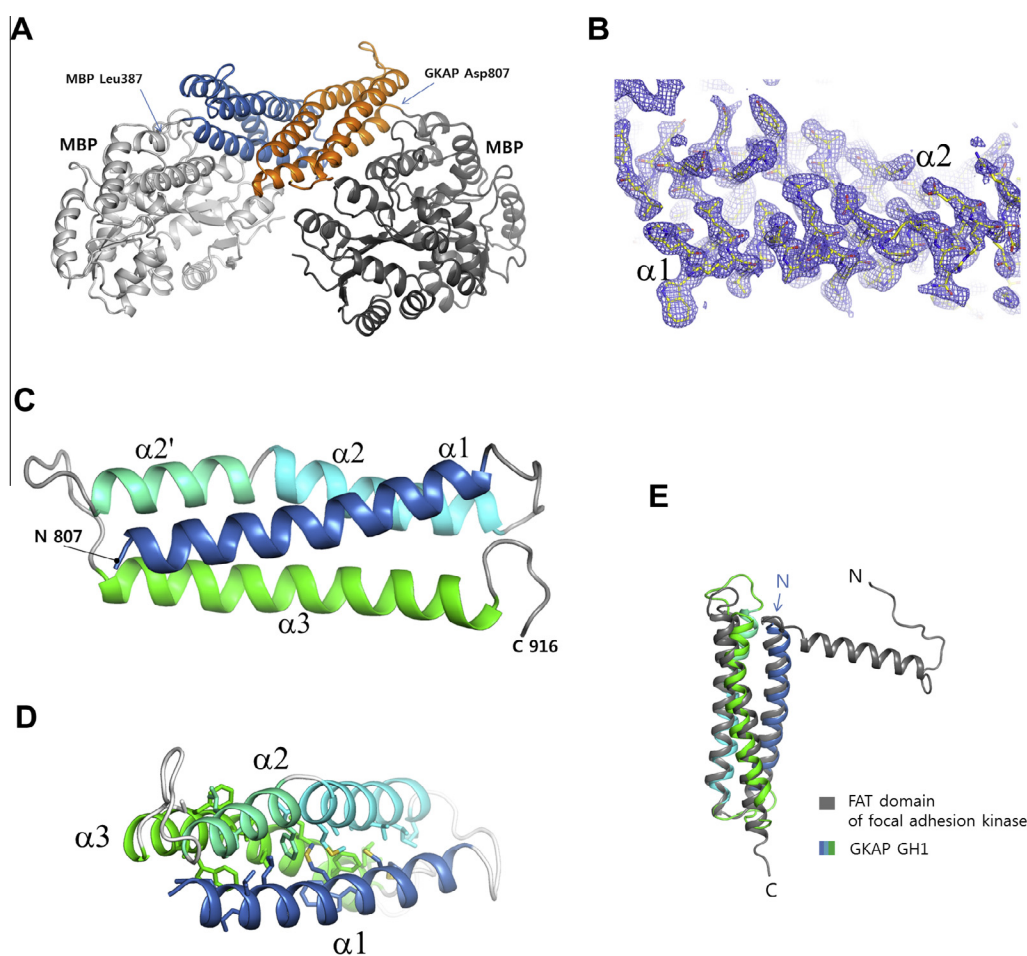


**Fig. 2.** Overall structure of GKAP GH1. (A) Overall structure of MBP-GKAP GH1 fusion protein. The two MBP molecules in the asymmetric unit were colored in light and dark gray respectively. (B) 2.0 Å 2Fo-Fc model maps superimposed with the final MBP-GKAP models. (C) Structure of GKAP GH1 domain ( $\alpha 1$ – $\alpha 3$ ). The helices were colored from blue to green based on secondary structure succession. (D) Hydrophobic core of GKAP GH1 domain. (E) Structural comparison of GKAP GH1 domain with the known structure (PDB code: 1K04) in the Protein Data Bank using the DALI server. (For interpretation of the references to color in this figure legend, the reader is referred to the web version of this article.)

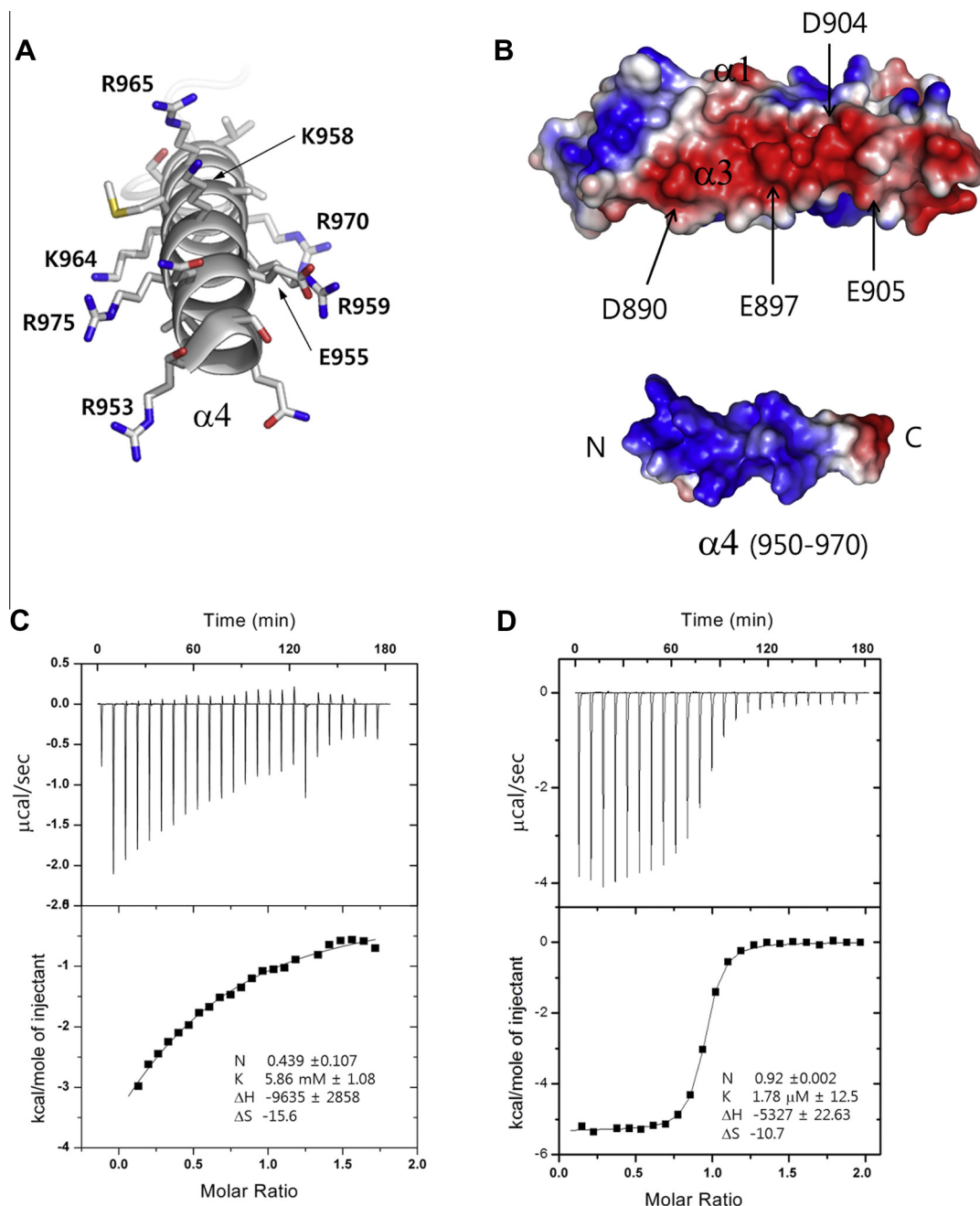


**Fig. 3.** Weak association of GKAP GH1  $\alpha 1$ – $\alpha 3$  with  $\alpha 4$ . (A) Amino acid arrangements of helix  $\alpha 4$ . The side chains of 21 amino acid residues were shown as stick models. (B) Electrostatic surface presentation of GKAP GH1  $\alpha 1$ – $\alpha 3$  and GH1  $\alpha 4$ . (C) Measurement of the binding of GKAP GH1  $\alpha 1$ – $\alpha 3$  to GH1  $\alpha 4$  by isothermal titration calorimetry. (D) Titration of Shank PDZ to GKAP CT ( $\alpha 4$  – PDZ binding motif) by isothermal titration calorimetry.

### 2.3. Isothermal titration calorimetry

For the analysis of protein–protein interaction by isothermal titration calorimetry (ITC), Shank PDZ domain (residues 584–690) from *R. norvegicus* cloned in the pET28b vector was expressed in *E. coli* and purified by Ni–NTA affinity and size exclusion chromatography. GKAP H4 (helix  $\alpha 4$ , residues 950–971) and GKAP CT (helix  $\alpha 4$ –PDZ binding motif, residues 950–992) were cloned to the pHMBP vector. GKAP H1–H3 ( $\alpha 1$ – $\alpha 3$ , residues 807–911) was cloned to the pHIS vector. The GKAP proteins were expressed and purified using the same procedure described for the MBP–GKAP GH1. Shank PDZ (1.6 mM, injectant), and MBP–GKAP CT (0.2 mM, placed in the sample cell) were dissolved in 20 mM Tris–HCl, pH 7.5, and 100 mM NaCl. Titrations of MBP–GKAP CT

(24 injections of 12  $\mu$ l) to Shank PDZ were performed at 25 °C using a VP-ITC Microcalorimeter (MicroCal), and data were analyzed using Origin software (Origin Lab). The association of GKAP  $\alpha 1$ – $\alpha 3$  with GKAP  $\alpha 4$  was measured by injecting GKAP H1–H3 protein in 20 mM Tris–HCl, pH 7.5 (1.55 mM, 24 injections) to MBP–GKAP H4 (0.2 mM) in the sample cell.

## 3. Results and discussion

### 3.1. Structure of GKAP GH1

GKAP1 protein, the longest isoform of rat GKAPs is composed of 992 residues. The N-terminal residues 1–298 are missing in five splicing variants out of six GKAP isoforms. The middle



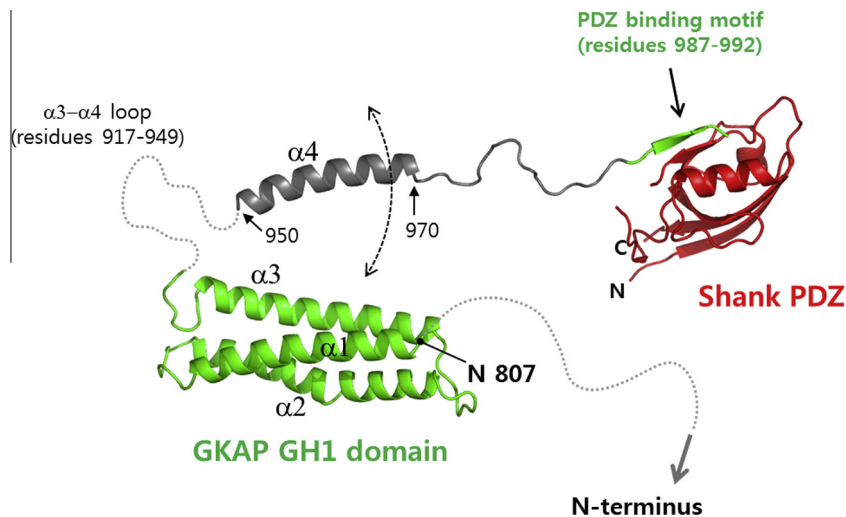


**Fig. 4.** The structural model of the GKAP C-terminal region. The helix  $\alpha 4$  was assigned based on the secondary structure prediction and modeled as a typical  $\alpha$ -helix. The connecting loop between  $\alpha 4$  and PDZ binding motif was modeled as a random loop. The structure of Shank PDZ – GKAP C-terminal peptide (PDB code: 1Q3P) was adapted from the previous work [19].

region spanning the residues 537–574 are absent in two isoforms. The GKAP isoforms have variable sequence in the residues 299–325. In contrast, all isoforms retain the GH1 domain and the several regions involved in synaptic protein interactions such as five 14 amino acid repeats (residues 343–503), the residues 665–698, the PDZ binding motif (Fig. 1A). Secondary structure prediction shows that GKAP is mostly unstructured except the C-terminal GH1 domain. GH1 domain is highly conserved in GKAP family members with 99% sequence identity of rat GKAP1 to human and mouse GKAP1. Rat GKAP1 GH1 shows 71% sequence identity to rat GKAP2. Due to the lack of secondary structures in the N-terminal region of GKAP, the C-terminal GH1 domain was selected for structural studies. GH1 domain (residues 807–970) is predicted to be composed of four  $\alpha$ -helices. A part of the longest  $\alpha 3$ - $\alpha 4$  loop (residues 917–945) rich in proline and lysine residues was truncated in the crystallized construct due to disorder and proteolysis of the loop (Fig. 1B) [11]. In addition, to improve the diffraction quality of GKAP GH1 crystals, maltose-binding protein was fused to the N-terminus of GKAP GH1.

The structure of GKAP GH1 was determined at 2.0 Å resolution by molecular replacement using MBP as a search model and the structure was refined to an *R* factor of 24.3% (Table 1). The final model contained two molecules of MBP-GKAP, 181 water molecules in the asymmetric unit (Fig. 2A). The three helices in the GH1 domains were clearly visible (Fig. 2B). The helix  $\alpha 4$  which is connected by the truncated  $\alpha 3$ - $\alpha 4$  loop to helix  $\alpha 3$  was invisible in the electron density maps probably due to disorder in the crystal lattice. GKAP GH1 domain is a monomer in solution. Two MBP GKAP molecules in the asymmetric unit were related by non-crystallographic twofold axis. Two GKAP GH1 protomers were almost identical in structure with the *C $\alpha$*  Rmsd of 0.72 Å between two molecules. The core of the GKAP GH1 ( $\alpha 1$ - $\alpha 3$ ) is composed of 110 amino acids. Three  $\alpha$  helices form a 50 Å long antiparallel helix bundle with flexible connecting loops (Fig. 2C). The interfaces between the three helices are composed exclusively by 25 hydrophobic residues (Fig. 2D). The second helix ( $\alpha 2$ - $\alpha 2'$ ) has a slight kink at Q859 by a hydrogen bonded turn in the middle of  $\alpha$ -helix. The three-helix bundle structure is stabilized by extensive hydrophobic interaction, three salt bridges, and two hydrogen bonds. The surface of GKAP GH1 domain is mostly hydrophilic and

exposes a small hydrophobic patch of 150 Å<sup>2</sup> in the cleft between  $\alpha 2$  and  $\alpha 3$ .

The GKAP GH has no amino acid sequence similarity to any characterized protein domains and to the proteins of known structures in the Protein Data Bank. GKAP GH1 displays a simple three-helix bundle structure and it does not contain a pocket on the protein surface to compose an active site for enzymatic function. As an alternative approach to obtain a clue for the domain function, we carried out structural comparison of GKAP GH1 domain with the structures in the PDB using DALI server. GKAP GH displays the highest structural homology with the Z score of 9.9 to the FAT domain of focal adhesion kinase 1 (PDB code: 1k04) (Fig. 2E). FAT domain is involved in protein targeting by protein-protein interaction [17]. Structural topology of GKAP GH and FAT are similar in overall. However, due to the sequence difference of two domains, functional insight could not be inferred from the structural comparison.

### 3.2. Association of helix $\alpha 4$ to the $\alpha 1$ - $\alpha 3$ of GKAP GH1 domain

The crystallized construct includes the residues 950–971 which are strongly predicted as a  $\alpha$ -helix ( $\alpha 4$ ). However, the helix  $\alpha 4$  could not be assigned in the electron density maps possibly due to the disorder of this region. The helix  $\alpha 4$  is composed of 21 amino acids with 7 positively charged residues and one acidic residue (Fig. 3A). We suppose that the helix  $\alpha 4$  does not form a stable helix bundle with the helix  $\alpha 1$ - $\alpha 3$  due to the weak binding affinity. Helices  $\alpha 1$ ,  $\alpha 2$ , and  $\alpha 3$  are held together by extensive hydrophobic and many electrostatic interactions. However, helix  $\alpha 4$  is mostly composed of hydrophilic residues. Electrostatic surface presentation of GKAP GH1 reveals that  $\alpha 3$  of GKAP GH1 has a negative electrostatic surface with three Asp residues (Fig. 3B). Helix  $\alpha 4$  displays a strong positive electrostatic potential which is opposite to that of helix  $\alpha 3$ . Therefore, it is conceivable that helix  $\alpha 3$  and  $\alpha 4$  have electrostatic interaction. To prove this hypothesis, we measure the binding affinity of helix  $\alpha 4$  and helix  $\alpha 1$ - $\alpha 3$  by isothermal titration calorimetry (Fig. 3C). Titration with GH1  $\alpha 1$ - $\alpha 3$  as an injectant to the MBP-GKAP H4 ( $\alpha 4$ , residues 950–971) displayed a clean binding isotherm with a weak binding affinity of 5.9 mM.

### 3.3. Binding of the C-terminal PDZ binding motif to Shank PDZ domain

GKAP isoforms associate with Shank proteins by their C-terminal PDZ binding motifs. GKAP PDZ binding motif is a classical type I substrate involving a Thr/Ser residue in the third position of PDZ binding motif. We measured the binding affinity of GKAP PDZ-binding motif to Shank PDZ domain (Fig. 3D). The residues 950–992 spanning helix  $\alpha 4$  and the C-terminal PDZ binding motif was fused to the N-terminal MBP. GKAP PDZ binding motif showed 1.8  $\mu\text{M}$  affinity to Shank PDZ which is slightly stronger than the affinity ( $K_d$  9.0  $\mu\text{M}$ ) to  $\beta\text{PIX}$  peptide [18].

### 3.4. Modeling of overall structure of the GKAP C-terminal region

To get an insight on the overall structure of GKAP protein, we build a schematic model showing domain association between GKAP GH1 and Shank PDZ (Fig. 4). GKAP GH1 domain contains a rigid core composed of a three-helix bundle. The fourth helix is connected to the GH1 core by a long disordered  $\alpha 3$ – $\alpha 4$  loop. The helix  $\alpha 4$  associates weakly with the GH1 core ( $\alpha 1$ – $\alpha 3$ ) with a high mobility. The C-terminal PDZ binding motif which associates with Shank PDZ is connected to the GH1 domain by a 37 Å long random loop. The modeling suggests that the connection of key domains by flexible loops seems to be efficient for the protein–protein interaction of multiple scaffolding proteins by providing flexible binding configurations.

In conclusion, we determined the structure of the GKAP GH1 domain displaying a three-helix bundle loosely associated with the helix  $\alpha 4$ . So far, despite the critical role of GKAPs in synaptic protein clustering and the strict conservation of GH1 domain in this protein family, the exact role of GH1 domain is still not known. Generally, the key domains and the motifs involved in protein–protein interaction are well conserved in synaptic scaffolding proteins for the proper targeting and clustering of synaptic proteins. This feature confers a more weight on the protein–protein interaction module as a probable role of the GH1 domain. Finally, this work provides a structural basis of the GH1 domain for the future studies on GKAP protein function.

## 4. PDB accession number

Coordinates and structure factors for the GKAP GH1 domain have been deposited at the Protein Data Bank with an accession code 4ROY.

## Acknowledgments

We would like to thank beamline staffs at PLS-5C and PLS-7A of Pohang Accelerator Laboratory. This research was supported by Basic Science Research Program through the National Research Foundation of Korea (NRF) funded by the Ministry of Science, ICT and Future Planning (Grant No. NRF-2011-0025110).

## References

- [1] S. Naisbitt, E. Kim, R.J. Weinberg, A. Rao, F.C. Yang, A.M. Craig, M. Sheng, Characterization of guanylate kinase-associated protein, a postsynaptic density protein at excitatory synapses that interacts directly with postsynaptic density-95/synapse-associated protein 90, *J. Neurosci.* 17 (1997) 5687–5696.
- [2] M. Sheng, C.C. Hoogenraad, The postsynaptic architecture of excitatory synapses: a more quantitative view, *Annu. Rev. Biochem.* 76 (2007) 823–847.
- [3] E. Kim, S. Naisbitt, Y.P. Hsueh, A. Rao, A. Rothschild, A.M. Craig, M. Sheng, GKAP, a novel synaptic protein that interacts with the guanylate kinase-like domain of the PSD-95/SAP90 family of channel clustering molecules, *J. Cell Biol.* 136 (1997) 669–678.
- [4] K. Hirao, Y. Hata, N. Ide, M. Takeuchi, M. Irie, I. Yao, M. Deguchi, A. Toyoda, T.C. Sudhof, Y. Takai, A novel multiple PDZ domain-containing molecule interacting with N-methyl-D-aspartate receptors and neuronal cell adhesion proteins, *J. Biol. Chem.* 273 (1998) 21105–21110.
- [5] S. Naisbitt, E. Kim, J.C. Tu, B. Xiao, C. Sala, J. Valtschanoff, R.J. Weinberg, P.F. Worley, M. Sheng, Shank, a novel family of postsynaptic density proteins that binds to the NMDA receptor/PSD-95/GKAP complex and cortactin, *Neuron* 23 (1999) 569–582.
- [6] S. Naisbitt, J. Valtschanoff, D.W. Allison, C. Sala, E. Kim, A.M. Craig, R.J. Weinberg, M. Sheng, Interaction of the postsynaptic density-95/guanylate kinase domain-associated protein complex with a light chain of myosin-V and dynein, *J. Neurosci.* 20 (2000) 4524–4534.
- [7] J.B. Manneville, M. Jehanno, S. Etienne-Manneville, Dlg1 binds GKAP to control dynein association with microtubules, centrosome positioning, and cell polarity, *J. Cell Biol.* 191 (2010) 585–598.
- [8] J.C. Tu, B. Xiao, S. Naisbitt, J.P. Yuan, R.S. Petralia, P. Brakeman, A. Doan, V.K. Aakalu, A.A. Lanahan, M. Sheng, P.F. Worley, Coupling of mGluR/Homer and PSD-95 complexes by the Shank family of postsynaptic density proteins, *Neuron* 23 (1999) 583–592.
- [9] A.Y. Hung, C.C. Sung, I.L. Brito, M. Sheng, Degradation of postsynaptic scaffold GKAP and regulation of dendritic spine morphology by the TRIM3 ubiquitin ligase in rat hippocampal neurons, *PLoS One* 5 (2010) e9842.
- [10] S.M. Shin, N. Zhang, J. Hansen, N.Z. Gerges, D.T. Pak, M. Sheng, S.H. Lee, GKAP orchestrates activity-dependent postsynaptic protein remodeling and homeostatic scaling, *Nat. Neurosci.* 15 (2012) 1655–1666.
- [11] J. Tong, H. Yang, Y.J. Im, Crystallization and preliminary X-ray crystallographic analysis of the C-terminal domain of guanylate kinase-associated protein from *Rattus norvegicus*, *Acta Crystallogr. F Struct. Biol. Commun.* 70 (2014) 949–954.
- [12] M.D. Winn, C.C. Ballard, K.D. Cowtan, E.J. Dodson, P. Emsley, P.R. Evans, R.M. Keegan, E.B. Krissinel, A.G. Leslie, A. McCoy, S.J. McNicholas, G.N. Murshudov, N.S. Pannu, E.A. Potterton, H.R. Powell, R.J. Read, A. Vagin, K.S. Wilson, Overview of the CCP4 suite and current developments, *Acta Crystallogr. D Biol. Crystallogr.* 67 (2011) 235–242.
- [13] A. Vagin, A. Teplyakov, Molecular replacement with MOLREP, *Acta Crystallogr. D Biol. Crystallogr.* 66 (2010) 22–25.
- [14] A.J. Sharff, L.E. Rodseth, J.C. Spurlino, F.A. Quioco, Crystallographic evidence of a large ligand-induced hinge-twist motion between the two domains of the maltodextrin binding protein involved in active transport and chemotaxis, *Biochemistry* 31 (1992) 10657–10663.
- [15] A.T. Brunger, P.D. Adams, G.M. Clore, W.L. DeLano, P. Gros, R.W. Grosse-Kunstleve, J.S. Jiang, J. Kuszewski, M. Nilges, N.S. Pannu, R.J. Read, L.M. Rice, T. Simonson, G.L. Warren, Crystallography & NMR system: a new software suite for macromolecular structure determination, *Acta Crystallogr. D Biol. Crystallogr.* 54 (1998) 905–921.
- [16] P. Emsley, B. Lohkamp, W.G. Scott, K. Cowtan, Features and development of Coot, *Acta Crystallogr. D Biol. Crystallogr.* 66 (2010) 486–501.
- [17] S.T. Arold, M.K. Hoellerer, M.E. Noble, The structural basis of localization and signaling by the focal adhesion targeting domain, *Structure* 10 (2002) 319–327.
- [18] Y.J. Im, G.B. Kang, J.H. Lee, K.R. Park, H.E. Song, E. Kim, W.K. Song, D. Park, S.H. Eom, Structural basis for asymmetric association of the betaPIX coiled coil and Shank PDZ, *J. Mol. Biol.* 397 (2010) 457–466.
- [19] Y.J. Im, J.H. Lee, S.H. Park, S.J. Park, S.H. Rho, G.B. Kang, E. Kim, S.H. Eom, Crystal structure of the Shank PDZ-ligand complex reveals a class I PDZ interaction and a novel PDZ-PDZ dimerization, *J. Biol. Chem.* 278 (2003) 48099–48104.